Journal of Alloys and Compounds 590 (2014) 465–468

Contents lists available at ScienceDirect

Journal of Alloys and Compounds

journal homepage: www.elsevier.com/locate/jalcom

Letter

Sonochemical synthesis and electrogenerated chemiluminescence properties of 8-hydroxyquinoline manganese (Mnq_2) nanobelts

Xiao-Dong Yang, Xi-Bao Chen, Chang-Jie Mao *, Ji-Ming Song, He-Lin Niu, Sheng-Yi Zhang

School of Chemistry and Chemical Engineering, Anhui University, Hefei 230039, PR China

ARTICLE INFO

Article history:
Received 13 June 2013
Received in revised form 21 November 2013
Accepted 10 December 2013
Available online 16 December 2013

Keywords:
8-Hydroxyquinoline manganese
Sonochemical synthesis
Electrogenerated chemiluminescence

ABSTRACT

8-Hydroxyquinoline manganese (Mnq_2) nanobelts with width of 500 nm and length of 2–4 μm have been synthesized by a facile sonochemical route. The composition, morphology and size of the as-prepared sample were confirmed by elemental analysis (EA), Fourier transform infrared spectroscopy (FT-IR), thermogravimetric analysis (TGA) and field-emission scanning electron microscopy (FE-SEM). The reaction parameters, such as the mole ratio of reactants and the concentration of ethylene glycol, play an important part in the morphology of the final product. The electrogenerated chemiluminescence (ECL) properties of the Mnq_2 sample with different morphologies have also been investigated. The ECL spectra show that the Mnq_2 nanobelts exhibited excellent electrogenerated chemiluminescence (ECL) behavior.

1. Introduction

Synthesis of functional nanomaterials is one of the crucial steps to produce realistic nanodevices applied in various fields such as field effect transistor, photoelectric, sensors, and catalysis [1,2]. It is well known that the composition, shape and size of nanomaterials are an important elements in varying their electrical, optical, and other properties. The same with inorganic nanomaterials, organic nanomaterials should also exhibits differentiated properties in relation to bulky materials [3–5]. Thus, more and more attention is turning to synthesis of organic nanomaterials with different morphologies. For example, polydioxythiophene nanodots, nanowires, nano-networks, and tubular structures were prepared through electropolymerization method on indium–tin–oxide substrates [6]. Greenish-yellow luminescent graphene quantum dots were synthesized via a facile microwave avenue [7]. However, the ability to tune the shapes of organic materials lags well behind and needs to be improved. Therefore, it is still a challenge to develop a simple and fast method to fabricate organic materials with desirable morphologies.

Metal 8-hydroxyquinoline chelates (Mq_n) have been studied extensively and widely applied to electroluminescence, photoluminescence and field-emission [8,9]. Anzenbacher group synthesized a series of emission-color-tunable Alq_3 complexes with arylethynyl substituents [10]. Gaq_3 might be used as a superior emitter materials for display applications [11]. Due to unique optoelectronic properties of organic nanomaterials, much attention is turning to Mq_n nanostructure. Alq_3 nanostructures, such as nanowires, nanorods, and nanocrystalline films, exhibited field emission with a relatively low turn-on voltage [12–14]. Cadmium 8-hydroxyquinoline chloride (CdqCl) nanowires have potential future application in glucose-sensing [15]. However, most research reports have focused on Alq_3 and Znq_2 nanostructures. Few studies have investigated the synthesis of other metal 8-hydroxyquinoline nanostructures. Here, 8-hydroxyquinoline manganese (Mnq_2) nanobelts are synthesized by a facile sonochemical route. The electrogenerated chemiluminescence property of the as-prepared Mnq_2 nanobelts shows excellent ECL behaviors.

2. Experimental section

2.1. Synthesis

All the chemical regents were used without further purification. In a typical procedure, 1 mmol 8-hydroxyquinoline (C_9H_7NO, Sinopharm Chemical Reagent Co., Ltd., Shanghai) and 0.5 mmol manganese acetate tetrahydrate ($Mn(CH_3COO)_2\cdot 4H_2O$, Tianjin Guangfu Fine Chemical Research Institute, Tianjin) were separately dissolved in 25 mL ethylene glycol (EG, Sinopharm Chemical Reagent Co., Ltd., Shanghai). The molar ratios of Mn/q is 1:2. The total volume of reactants is 50 mL and the second solvent is distilled water. The solutions were mixed and exposed to high-intensity ultrasound irradiation under ambient air for 45 min. Ultrasound irradiation was accomplished with a high-intensity ultrasonic probe (Xinzhi Co., China, JY92-2D, 10 mm diameter; Ti-horn, 20 kHz, 80 W/cm^2) immersed directly in the reaction solution. After cooling the sample to room temperature, the precipitate was separated by centrifuging at a rotation rate of 9000 rpm. Then, it was washed with distilled water and absolute ethanol in sequence, and dried in air at room temperature.

2.2. Measurements

Element analysis (EA) was obtained on a Vario EL III elemental analyzer. Fourier transform infrared spectroscopy (FT-IR) was conducted by a Nicolet NEXUS 870 FT-IR spectrophotometer. The thermogravimetric analysis (TGA) was carried out on a Netzsch STA 449F3 thermal analysis device. TGA determination was carried out

---

* Corresponding author. Tel./fax: +86 551 63861279.
E-mail address: maochangjie@sina.com (C.-J. Mao).

0925-8388/$ - see front matter © 2014 Published by Elsevier B.V.
http://dx.doi.org/10.1016/j.jallcom.2013.12.089

in air at a heating rate of 10 °C/min in a range of room temperature to 800 °C. Field-emission Scanning electron microscopy (FE-SEM) images were taken using a Hitachi S-4800 scanning electron microscope. The ECL experiments were conducted by LK2005A electrochemistry work station and Remax RFL-1A chemiluminescence analyzer with a conventional three-electrode system composed of a platinum wire as the auxiliary electrode and a Ag/AgCl electrode as the reference; working electrodes were Mnq_2 nanobelts modified glass carbon electrodes (GCE, 4 mm diameter), respectively.

3. Result and discussion

The component of the as-synthesized product was confirmed by EA. The result revealed that the weight of C, N, and H were 62.98%, 8.16%, and 3.52%, respectively. The experimental data is good agreement with the calculated values (C: 61.76; N: 8.03; H: 3.48 wt.%). The composition of the final sample was further proved by spectroscopy measurement. In the FTIR spectrum of Mnq_2 (Fig. 1a), the bands about 1600–744 cm^{-1} are attributed to C=C, CC/CN, CH, CH/CCN, CN/CO functional groups of the quinoline group. The peaks at 643, 599 and 559 cm^{-1} are correspond to Mn—O stretching vibration and the peaks at 498 cm^{-1} are assigned to Mn—N stretching vibration. The above results are in good agreements with Mnq_2 [16,17]. The TGA result (Fig. 1b) indicated that the final remaining weight was about 22.93%, which agreed well with the theoretical weight surplusage of Mn_2O_3 (23.03%) produced from the reaction between Mnq_2 and O_2 in air. Therefore, it was obvious that the metal–ligand molar ratios is 1:2. So the chemical composition of final product could be confirmed to be $Mn(C_9H_7NO)_2$.

The morphology and size of the Mnq_2 sample were observed by FE-SEM. Fig. 1c clearly demonstrates that Mnq_2 shows a large quantity of nanobelts with width of 500 nm and length of 2–4 μm. Furthermore, a high-magnification SEM image (Fig. 1d) revealed that their average thickness is about 200 nm. When the $Mn(Ac)_2/q$ ratio was changed in the range from 1:2 to 4:2, no significant changes in the final morphology. However, when $Mn(Ac)_2/q$ ratio decreased to 1:5, only aggregated flake morphology are observed (Fig. 1e).

The concentration of ethylene glycol plays an important role in the morphology of the final product. If the concentration of EG is 10 vol%, irregular sheet-like morphology with the size of 2 μm is formed. In addition, some particles are observed in the final sample (Fig. 2a). With increase the concentration of EG to 30 vol%, the obtained Mnq_2 is composed of a large quantity of irregular sheet (Fig. 2b). When the concentration of EG was changed to 90 vol%, nanoblets with a wide size distribution was observed (Fig. 2c). When 100 vol% EG was used, a regular nanobelts with mean diameter of 1 μm was observed (Fig. 2d). In EG solution, Mn(II) ions are surrounded and protected by EG molecules, and forming the

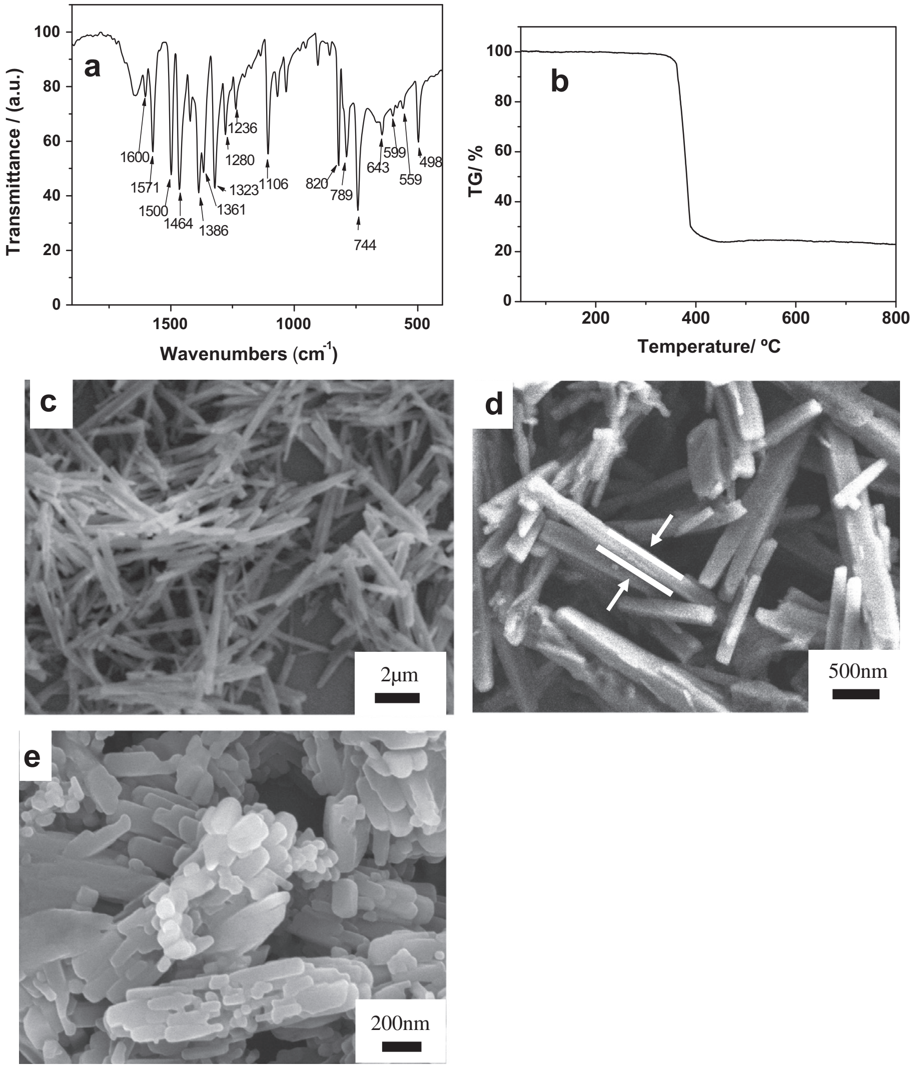

Fig. 1. (a) FTIR spectrum, (b) TGA, (c) SEM image and (d) a high-magnification SEM image of the Mnq_2 sample synthesized at Mn/q ratio of 1:2; and (e) SEM images of Mnq_2 sample synthesized at Mn/q ratio of 1:5.

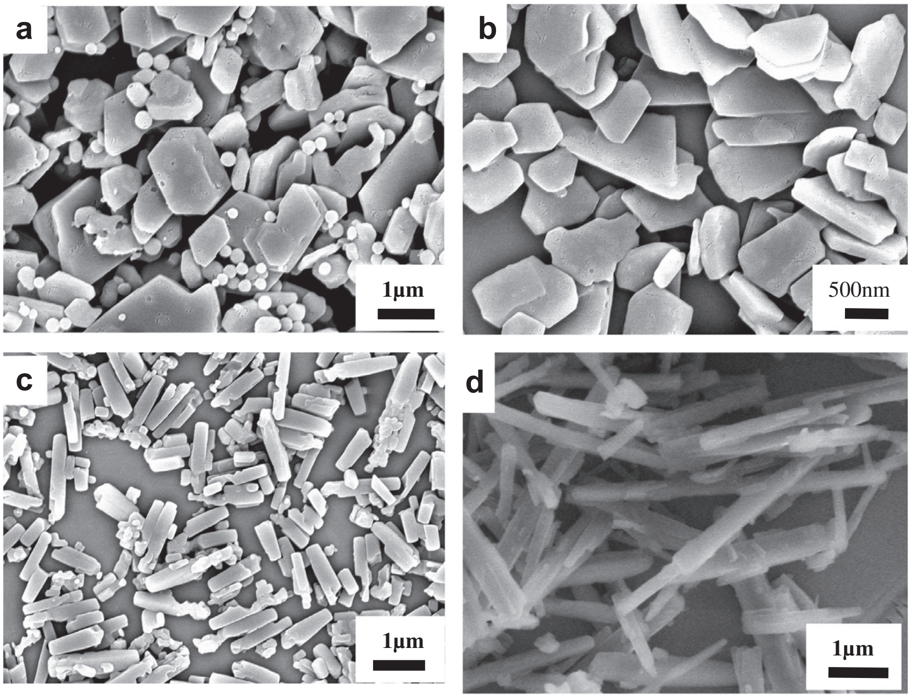

Fig. 2. SEM images of Mnq_2 prepared with the EG concentration of (a) 10 vol%, (b) 30 vol%, (c) 90 vol%, and (d) 100 vol%.

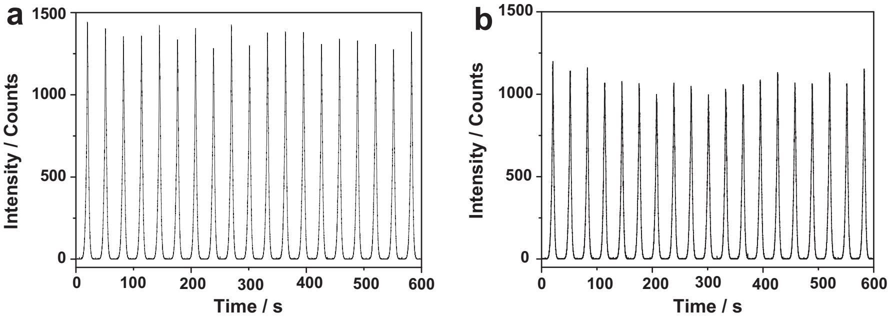

Fig. 3. ECL emission spectra from the Mnq_2 (a) nanobelts and (b) sheet-like morphology in 0.1 M PBS containing 0.1 M KCl, 0.1 M $K_2S_2O_8$ under a cyclic voltammetry scan rate of 100 mV/s.

complexes with one or more ethylene glycol ligands [18,19]. 8-Hydroxyquinoline might be selectively adsorbed onto some surfaces of the Mnq_2 crystals through O—Mn bonding. This could resulting in formation of 1D nanostructures in a particular direction.

In our work, the ECL behaviors of Mnq_2 with different morphologies were studied. The ECL emission spectra is shown in Fig. 3. The electrode potential was cycled between 0.0 and −1.6 V at a scanning rate of 100 mV s^{-1} for 16 cycles. The Mnq_2 sample, as a novel ECL reagent, shows good ECL light emission. In our case, ECL is produced upon concomitant reduction of Mnq_2 and $S_2O_8^{2-}$. Upon the potential scan with negative direction, the Mnq_2 crystal was reduced to anion radicals ($Mnq_2^{-\cdot}$). Simultaneously, $S_2O_8^{2-}$ was oxidized to produce a strong oxidant $SO_4^{-\cdot}$, then $Mnq_2^{-\cdot}$ can react with $SO_4^{-\cdot}$ to emit light in aqueous solution. The proposed ECL mechanism is as follows:

$$Mnq_2 + e^- \rightarrow Mnq_2^{-\cdot} \quad (1)$$

$$S_2O_8^{2-} + e^- \rightarrow SO_4^{2-} + SO_4^{-\cdot} \quad (2)$$

$$Mnq_2^{-\cdot} + SO_4^{-\cdot} \rightarrow Mnq_2^{*} + SO_4^{2} \quad (3)$$

$$Mnq_2^{*} \rightarrow Mnq_2 + h\nu \quad (4)$$

The ECL light emissions of all samples exhibited quite stability intensity. Obviously, the ECL emission intensity of Mnq_2 nanobelts is much higher than that of sheet-like Mnq_2, which indicate the morphologies of the final sample could affect the ECL emission. Some previously research reports have proved that the ECL emission is dependent on the surface properties and the presence of surface defects [20,21]. The difference may be attribute to the more surface defects of the Mnq_2 nanobelts caused by faster crystal formation would emit stronger ECL emission. The above results suggested that the Mnq_2 nanobelts had great potential applications in biosensor and biomarker.

4. Conclusions

In this paper, we have successfully synthesized Mnq_2 nanobelts using a simple and facile sonochemical route. The electrogenerated chemiluminescence properties of the as-prepared Mnq_2 nanobelts were investigated. The results indicated that the Mnq_2 nanobelts have excellent ECL behavior. The relatively strong ECL behavior from the Mnq_2 of will provide potential applications in ECL biosensors and for bio-labelling.

Acknowledgments

This work was supported by Natural Science Foundation of Anhui Province (11040606Q02), State Key Laboratory of Analytical Chemistry for Life Science (SKLACLS1204), 211 project of Anhui University, the National Natural Science Foundation of China (Grant No. 21071002, 21275006) and Key Project of Anhui Provincial Education Department (KJ2013A029).

References

[1] C.P. Collier, R.J. Satkally, J.J. Shiang, S.E. Henrichs, J.R. Heath, Science 277 (1997) 1978.
[2] V.F. Punters, K.M. Krishnan, A.P. Alivisatos, Science 291 (2001) 2115.
[3] H.B. Fu, J.N. Yao, J. Am. Chem. Soc. 123 (2001) 1434.
[4] H.P. Cong, S.H. Yu, Adv. Funct. Mater. 18 (2008) 195.
[5] J.S. Hu, H.X. Ji, A.M. Cao, Z.X. Huang, Y. Zhang, L.J. Wan, A.D. Xia, D.P. Yu, X.M. Meng, S.T. Lee, Chem. Commun. 29 (2007) 3083.
[6] S.C. Luo, J. Sekine, B. Zhu, H.C. Zhao, A. Nakao, H.H. Yu, ACS Nano 6 (2012) 3018.
[7] L.L. Li, J. Ji, R. Fei, C.Z. Wang, Q. Lu, J.R. Zhang, L.P. Jiang, J.J. Zhu, Adv. Funct. Mater. 22 (2012) 2971.
[8] C.W. Tang, S.A. VanSlyke, Appl. Phys. Lett. 51 (1987) 913.
[9] M. Cöle, J. Gmeiner, W. Milius, H. Hillebrecht, W. Brütting, Adv. Funct. Mater. 13 (2003) 108.
[10] R. Pohl, P. Anzenbacher, Org. Lett. 5 (2003) 2769.
[11] L.S. Sapochak, A. Padmaperuma, N. Washton, F. Endrino, G.T. Schmett, J. Marshall, D. Fogarty, P.E. Burrows, S.R. Forrest, J. Am. Chem. Soc. 123 (2001) 6300.
[12] J.J. Chiu, C.C. Kei, T.P. Perng, W.S. Wang, Adv. Mater. 15 (2003) 1361.
[13] J.S. Hu, H.X. Ji, A.M. Cao, Z.X. Huang, Y. Zhang, L.J. Wan, A.D. Xia, D.P. Yu, X.M. Meng, S.T. Lee, Chem. Commun. (2007) 3083.
[14] J.J. Chiu, W.S. Wang, C.C. Kei, C.P. Cho, T.P. Perng, P.K. Wei, S.Y. Chiu, Appl. Phys. Lett. 83 (2003) 4607.
[15] H.C. Pan, H.Y. Lin, Q.M. Shen, J.J. Zhu, Adv. Funct. Mater. 18 (2008) 3692.
[16] C.L. Lu, Z.H. Fu, Y.C. Liu, F.L. Liu, J.W. Qin, X.L. He, D.L. Yin, Acta Phys. Chim. Sin. 26 (2010) 2705.
[17] A.K. Nakamoto, Infrared and Raman Spectra of Inorganic Coordination Compounds, Wiley-Interscience Publication, New Jersey, 1975.
[18] Y.L. Wang, X.C. Jiang, Y.N. Xia, J. Am. Chem. Soc. 125 (2003) 16176.
[19] J. Geng, X.D. Jia, J.J. Zhu, Nanotechnology 17 (2006) 2614.
[20] Z. Ding, B.M. Quinn, S.K. Haram, L.E. Pell, B.A. Korgel, A.J. Bard, Science 296 (2002) 1293.
[21] N. Myung, Z. Ding, A.J. Bard, Nano Lett. 2 (2002) 1315.